AD-A070 670 CASE WESTERN RESERVE UNIV CLEVELAND OHIO DEPT OF MACR--ETC F/G 11/9
RELATIONSHIPS BETWEEN MECHANICAL BEHAVIOR AND CRAZE MORPHOLOGY --ETC(U)
JUN 79 J S TRENT, I PALLEY, E BAER N00014-75-C-0795

UNCLASSIFIED TR-9 NL

| OF |
AD
A070670

END
DATE
FILMED
8-79
DDC

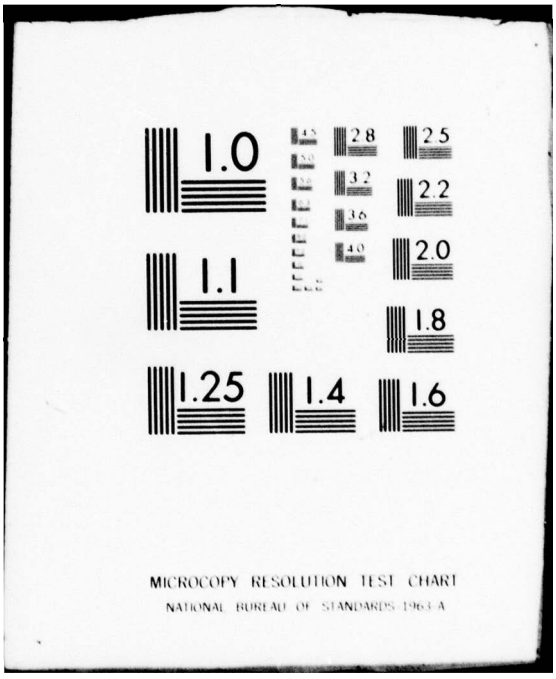
1.0
1.1
1.25
1.4
1.6
2.8
3.2
3.6
4.0
2.5
2.2
2.0
1.8
MICROCOPY RESOLUTION TEST CHART
NATIONAL BUREAU OF STANDARDS-1963-A

AD A070670

DDC FILE COPY

SECURITY CLASSIFICATION OF THIS PAGE (When Data Entered)

REPORT DOCUMENTATION PAGE

READ INSTRUCTIONS BEFORE COMPLETING FORM

1. REPORT NUMBER: Technical Report #9	2. GOVT ACCESSION NO.
3. RECIPIENT'S CATALOG NUMBER	
4. TITLE (and Subtitle): RELATIONSHIPS BETWEEN MECHANICAL BEHAVIOR AND CRAZE MORPHOLOGY IN THIN FILMS OF POLYSTYRENE	5. TYPE OF REPORT & PERIOD COVERED: Technical Report/Interim rept.
	6. PERFORMING ORG. REPORT NUMBER
7. AUTHOR(s): J. S. Trent, I. Palley and E. Baer	8. CONTRACT OR GRANT NUMBER(s): N00014-75-C-0795
9. PERFORMING ORGANIZATION NAME AND ADDRESS: Department of Macromolecular Science, Case Western Reserve University, Cleveland, Ohio 44106	10. PROGRAM ELEMENT, PROJECT, TASK AREA & WORK UNIT NUMBERS: 39p.
11. CONTROLLING OFFICE NAME AND ADDRESS: Office of Naval Research (Code 472), Arlington, Virginia 22217	12. REPORT DATE: 20 June 1979
	13. NUMBER OF PAGES
14. MONITORING AGENCY NAME & ADDRESS (if different from Controlling Office): TR-9	15. SECURITY CLASS. (of this report): Unclassified
	15a. DECLASSIFICATION/DOWNGRADING SCHEDULE

LEVEL II

16. DISTRIBUTION STATEMENT (of this Report)

Approved for public release; distribution unlimited. Reproduction in whole or in part is permitted for any purpose of the United States Government.

17. DISTRIBUTION STATEMENT (of the abstract entered in Block 20, if different from Report)

DDC RECEIVED JUL 2 1979 C

18. SUPPLEMENTARY NOTES

19. KEY WORDS (Continue on reverse side if necessary and identify by block number)

Polystyrene, Glassy polymer, Craze, Morphology Mid-rib, Formation, Thin film, Electron microscope, Stress, Strain, Strain rate, Thermal history, Annealing, Mechanistic model.

20. ABSTRACT (Continue on reverse side if necessary and identify by block number)

A new technique has been developed to study the relationship between mechanical properties and craze microstructure in thin films (1-10μm) of polystyrene. These thicknesses allowed us to strain the films in a conventional testing machine and subsequently examine them in the deformed state in an electron microscope. Strain rate was systematically varied and its effect was investigated on both quenched and annealed samples. correlations were found between craze morphology and ductility.

DD FORM 1 JAN 73 1473 EDITION OF 1 NOV 65 IS OBSOLETE S/N 0102-014-6601 |

SECURITY CLASSIFICATION OF THIS PAGE (When Data Entered)

408 357

A new 'craze parameter' fundamental to our theoretical interpretation has been defined as the width of a strip of material which is involved in the development of a craze. From this value, the average strain and the average volume fraction of fibrils within a craze can be calculated. In order to obtain a mechanistic model which is consistent with observed data, a changing relative local strain rate during craze formation had to be assumed.

Accession For
NTIS GRA&I
DDC TAB
Unannounced
Justification
By
Distribution/
Availability Codes
Dist | Avail and/or special
A

CASE WESTERN RESERVE UNIVERSITY
Department of Macromolecular Science
Cleveland, Ohio 44106

Technical Report No. 9

RELATIONSHIPS BETWEEN MECHANICAL BEHAVIOR AND CRAZE MORPHOLOGY IN THIN FILMS OF POLYSTYRENE

by

J. S. Trent, I Palley and E. Baer
Department of Macromolecular Science
Case Western Reserve University
Cleveland, Ohio 44106

June 20, 1979

Research Sponsored by the
Office of Naval Research

Contract N000014-75-C-0795

79 06 29 011

SYNOPSIS

A new technique has been developed to study the relationship between mechanical properties and craze microstructure in thin films (1-10μm) of polystyrene. These thicknesses allowed us to strain the films in a conventional testing machine and subsequently examine them in the deformed state in an electron microscope. Strain rate was systematically varied and its effect was investigated on both quenched and annealed samples. Correlations were found between craze morphology and ductility.

A new "craze parameter" fundamental to our theoretical interpretation has been defined as the width of a strip of material which is involved in the development of a craze. From this value, the average strain and the average volume fraction of fibrils within a craze can be calculated. In order to obtain a mechanistic model which is consistent with observed data, a changing relative local strain rate during craze formation had to be assumed.

79 06 29 011

1. INTRODUCTION

The degree of brittleness in glassy polymers is mainly determined by the generation of crazes propagating perpendicularly to an applied stress [1,2]. It is also accepted that crazes develop in regions of localized inhomogeneities within the material or at stress-raising flaws. However, a study of the literature indicates that there is no agreement among authors beyond these elementary points.

Gent [3] proposed that the dilatant stress component at the tip of a flaw can be high enough to transform glassy material into the rubbery state. The devitrified polymer cavitates under negative pressure and forms a craze. Sternstein and Ongchin [4] and Rusch and Beck [5] proposed that the dilatational stress field increases molecular mobility by increasing the free volume. Haward [6] and Andrews and Bevan [7] argue that the controlling parameter for craze formation is the hydrostatic cavitational stress for void growth. While Haward [6] and Argon [8] proposed that voids nucleate in clusters rather than singly ahead of the craze tip. At some critical value of porosity the voids become interconnected. They suggested that because of these interconnections the hydrostatic cavitational stress is lower than the yield stress. In support of this view, Wellinghoff and Baer [9] showed that the surface microstructure of thin films was sufficiently

heterogeneous to initiate localized strain inhomogeneities of approximately 300 Å in diameter. These localized zones ultimately coalesced along the minor principal stress direction. The formation of narrow disk-shaped plastic zones propagating perpendicular to the applied strain was described. Olf and Peterlin [10] modified Gent's proposal by stating that the negative pressure at a flaw reduces only the yield stress of the polymer at that point.

Though these authors [3-10] disagree on how crazes initiate, they all agree that crazes ultimately form by cavitation under some hydrostatic stress produced within the polymer at various stress raising flaws. Little is known about the distribution of stress and strains within a single craze. This lack of knowledge complicates any attempts to explain mechanisms of craze formation. Since craze formation has been based largely on void formation and free volume criteria, it was surprising to find that no study has been done relating craze morphology to variations in thermal history. By varying the "free volume" content, we can gain a better understanding of the proposed mechanisms for craze formation. We have developed a technique to study the relationship between the mechanical properties and craze microstructure in thin films of polystyrene. In addition, a systematic investigation showing the effect of thermal history on polystyrene has been carried out.

Wellinghoff and Baer [9], Beahan, Bevis and Hull [11], and Kramer [12], have studied the initiation and growth of crazes by examining strained PS thin films having thicknesses of 500 to 7500Å using transmission electron microscopy (TEM). Polystyrene films used in this study are between 2.3 and 2.7 μm thick. Many advantages are realized when this increased thickness is employed. Specimens cut from these films are sufficiently strong to support themselves without substrate and this fact enables their stress-strain behavior to be readily recorded. Crazes can grow freely through the film and are influenced only by other crazes, impurities, or defects within the PS matrix. Previous studies of craze microstructure were done by microtoming strained bulk specimens to obtain crazed samples thin enough for TEM. However, microtoming can cause craze fibril distortion. Although the films used in this study are near the upper limit of thickness for use in the electron microscope, they can be examined directly and produce high resolution micrographs.

Mechanisms explaining craze growth have received insufficient attention. There is no agreement on the mechanisms by which a craze thickens as it increases in length. Two possible thickening mechanisms for craze growth have been proposed. Verhyelpen-Heymans and Bauwens [13] have suggested that the thickening of the craze is due to creep of craze material. They postulate that no material is drawn into the craze during its growth. This mechanism has been termed fibril creep by Kramer [12].

Kramer argues that this mechanism is not dominant in the thickening of crazes. He believes that crazes thicken mainly by drawing new polymer from the polymer matrix into the craze. Beahan, Bevis and Hull [11] suggest that, at low strain-rates, crazes increase in thickness by the drawing of further matrix material into the craze and to some extent by an increase in the orientation of the fibrils.

To investigate the proposed mechanisms, the width of material in the unstressed film that finally is involved in the formation of the craze must be measured. By using the thin-film technique described in this paper, we have been able to determine this width. Also, it was possible to calculate values of the average strain and volume fraction of fibrils within a single craze.

2. EXPERIMENTAL

2.1. Film Preparation and Deformation

Solvent-cast thin films of general purpose atactic polystyrene (PS), generously supplied by Dow Chemical Company, were prepared as follows. A thirteen percent solution by weight of PS in O-xylene was prepared. Thin films (2.0-2.7 μm thick) were cast by dipping clean glass slides into the solution and then evaporating the solvent. The evaporation was performed by immediately placing the coated glass slides in a vacuum oven for one hour at room temperature and subsequently raising the temperature slowly to 70°C. Solvent removal was continued at this temperature for an additional twelve hours.

Before the thin-film was removed from a glass slide, it was cut with a razor blade into the shape illustrated in Figure 1(a) using a metal template as a guide. This design was chosen to avoid premature failure in the grips. The residual stress left along the edges of the tensile specimen (after cutting) was relieved by annealing on the glass slide for twelve hours at 105°C under vacuum. No trace of o-xylene could be detected in the film using Fourier Transform Infrared spectroscopy (FTIR) for detection after this final step.

To study the effect of thermal history on the mechanical properties and craze microstructure, samples were either slowly cooled to room temperature at a rate of 13°C/hr. (annealed) or quenched in an ice water bath (quenched) both from 105°C. After such thermal treatment, the specimens were removed from the glass slides by floatation on the surface of a water bath, and subsequent drying on filter paper.

The PS specimens were strained in tension using a conventional Instron testing machine. A sensitive load cell was used which gave a full-scale range of 20 grams. Due to accuracy limitations inherent in this type of experiment, meaningful modulus data could not be obtained. For this reason, only the craze initiation stress, the upper yield stress, the fracture stress, and the ultimate elongation are reported. The strain rates were 0.002, 0.008, 0.02, and 0.2 in./min for the annealed specimens, and were 0.02, 0.10, 0.20 and 0.5 in./min. for the quenched specimens. Accurate thickness determinations were made

by following the method described by Tolansky [14] using Fourier Transform Infrared.

2.2. Preparation of Specimens for Transmission Electron Microscopy

Specimens for viewing in the Transmission Electron Microscope (TEM) were strained to approximately 0.8% and removed from the Instron in the stressed state. This was done by quickly sandwiching the sample between two glass plates, one of which contained two strips of double-stick tape. Ultimately, stress relaxation did occur, but this technique kept the fine craze microstructure from reorienting. To insure dimensional stability for viewing in the electron microscope, a thin coating of platinum metal and carbon was shadowed onto the surface. The platinum metal gave good contrast for examination of the craze micro-structure. With an optical microscope, selected areas of the stressed specimens were cut and placed between 100 mesh folding copper grids, and subsequently observed in a Hatachi HU-11A electron microscope.

2.3. Thickness Determination of Material in the Craze

The width of a strip of material finally involved in a craze, W_o, was determined by evaporating gold onto the surface through a 400 mesh copper grid. Then these specimens were strained (Figure 1b), and lightly coated with carbon. Carbon improves contrast and also conducts away some of the heat produced by the electron beam.

To understand the experimental technique for the determination of W_o, consider first the schematic drawings in Figures 2 and 3 which show the results of both a crack and craze which have propagated through the tilt edge of a shadowed zone. Figure 2(a) represents the condition before stress is applied. The dashed line indicates the direction of a line along which a crack will propagate, and the shadowed zone is tilted ϕ degrees to the direction of crack propagation. When stress is applied (Figure 2(b)), the shadowed zone is separated due to the propagation of the crack by a distance equal to the crack width, W_f. Since a crack contains no material, W_o=O, all points along the line of progagation will separate in a vertical fashion with respect to each other a distance of W_f, as illustrated in (Figure 2(a,b)).

A craze, unlike a crack, contains material; so one must consider how this shadowed zone will separate with craze propagation. Figure 3(a) shows the condition before stress is applied. We will assume that all material between the dashed lines will ultimately make up the observed craze and also the material outside the dashed lines will not be involved in craze formation. Therefore, W_o is defined as the width between the dashed lines. The shadowed zone is tilted at angle ϕ to the boundary of the bottom dashed line. By measuring Δ, the horizontal length between points A and A^1, W_o can be determined by

$$W_o = \Delta \tan \phi. \qquad (1)$$

Once stress is applied (Figure 3(b)), the shadowed zone will deform, but not as if a crack had propagated through it. The shadowed area between the dashed lines will become less dense, due to deformation of involved material. One can see that Δ never changes as long as the material between the dashed lines elongates. If a measure of ϕ, Δ and W_f (final craze width) is made after deformation, then the average strain within the craze ($\bar{\varepsilon}_c$) and the average volume fraction of craze fibrils ($\bar{V}_f$) can be calculated by

$$\bar{\varepsilon}_c = \ln \frac{W_f}{W_o} \quad \text{and} \quad (2)$$

$$\bar{V}_f = \frac{W_o}{W_f} \, . \quad (3)$$

This experiment was performed on both annealed and quenched samples.

3. RESULTS

3.1. Effect of Thermal History and Strain Rate on Stress-Strain Behavior

Figure 4(a) shows the stress-strain behavior at various strain rates for the annealed thin films of PS tested in tension. The curves in Figures 4(a) and (b) are an average of at least three runs. At strain rates of 0.002, 0.008 and 0.02 in./min., the thin films exhibited ductile behavior and showed distinct yield points. As the strain rate increased, the elongation to break decreased while the craze initiation stress, yield stress

and fracture stress increased. Craze initiation occurs at the stress which corresponds to the onset of non-linearity on the stress-strain curve. At a strain rate of 0.2 in./min. the films fractured in a brittle manner.

Figure 4(b) shows the stress-strain curves with various strain-rates for thin film specimens rapidly quenched from their annealing temperatures. At strain rates of 0.02, 0.10 and 0.20 in./min., these films exhibited ductile behavior and showed distinct yield points. As in Figure 4(a) the elongation to break decreased and the craze initiation stress, yield stress and fracture stress increased with increasing strain rate. At a strain rate of 0.5 in./min. the films exhibited brittle fracture.

Ductility for both annealed and quenched material was attributed mainly to the formation of crazes which grow perpendicularly to the direction of applied stress. This can be clearly seen in Figure 5, which is an optical micrograph showing the gauge area of a quenched thin film strained at $\dot{\varepsilon}$ = 0.02 in./min. Photo (a) was taken with the polarizers parallel to each other, and photo (b) shows the craze film between crossed polarizers. The arrow indicates the direction of applied stress. Crazing seems to be the only deformation mechanism and is responsible for the observed ductility seen in Figures 4(a) and (b). Nielson [15] has given a description of how crazes can be responsible for large elongations in polymers. It is apparent that the yield stress, fracture stress

and craze initiation stress for the annealed specimens were considerably higher than those of the quenched specimens deformed under equal strain rates. However, at a given strain rate, the elongation to break was much larger for the quenched thin films than for those which were annealed. At $\dot{\varepsilon}$ = 0.02 in./min., the quenched specimens had a maximum elongation of approximately 2.8% while that of the annealed specimens was approximately 1.2%. A ten fold increase in the strain rate for the annealed material produced brittle behavior. In contrast, the quenched films remained ductile, although a ten-fold increase in strain rate greatly reduced the elongation to break.

Based on these results, it appears that by increasing strain rate or by annealing, the tendency toward brittle behavior is increased. However, these results alone cannot explain why the quenched material is more ductile than the annealed material. A detailed look at craze morphology as related to the observed mechanical properties for both annealed and quenched samples provided a deeper insight into this problem.

3.2. Effect of Thermal History and Strain Rate on Craze Morphology

An electron micrograph of a typical craze formed in an annealed sample is shown in Figure 6(a). This particular sample was strained at $\dot{\varepsilon}$ = 0.02 in./min. and drawn to break, and the craze shown was in the "mature" region several hundred microns from the craze-tip. The width of such crazes averaged approximately 2μm. A common characteristic of many crazes was a pronounced "void" region near the center of the craze having

an average width of about 2000Å. The polymer within this void region appears to be a three dimensional array of interconnected fibrils with diameters ranging between 200 to 500Å. This type of voiding was observed by Beahan et. al. [16] in crazes formed in thin films that were similarly prepared. Fine fibrils 200 to 400Å wide can be observed on either side of this void region. However, this fine structure does not traverse the entire width of the craze. Beahan et. al [16] have defined this void area as the midrib section of the craze. We will define the midrib region as the width of the observable fine fibrillar structure plus the width of the void region, if present. This definition was adopted because all crazes contained a region of fine fibrillar structure, but did not necessarily contain a void region. It is possible that in annealed materials voiding of the midrib area occurs just before fracture.

Figure 6(b) shows an electron micrograph of a typical craze formed in films quenched into ice water from a temperature of 105°C. This sample was strained at $\dot{\varepsilon}$ = 0.02 in./min. and drawn to break. Again, this micrograph was obtained from a region several hundred microns from the craze-tip. The widths of these crazes ranged from 3.4-4.0μm. As was observed for the annealed case, fine fibrils normal to the craze boundaries nearly spanned the entire width of the craze. This fibril-type structure had a uniform width averaging 350Å, and had no noticeable void region between fibrils. The fibrils were more distinguishable along the center of the craze and became less pronounced near the craze-matrix interface.

3.3. Craze Morphology and Ductility

Examination of the stress strain curves in Figure 4 reveals that samples quenched in ice-water elongated 2.5 times more than the samples slowly cooled to room temperature. This effect is reflected in the final craze widths. The "quenched" crazes were approximately 2 times wider than the "annealed" crazes. However, the fibrils within the midrib region for both types of crazes were similar in width and appearance. The most pronounced difference was the appearance of a void region within the midrib section of the "annealed" crazes. This void region never occurred in the quenched films strained at $\dot{\epsilon}$ = 0.02 in./min. The midrib width of "quenched" crazes was approximately 2.5 times larger than that of the "annealed" crazes. Quenching the thin films seems to have decreased the propensity for void growth in the midrib region and increased the uniformity of deformation.

A series of electron micrographs of crazes formed in films quenched from 105°C are shown in Figure 7. These micrographs are from the mature region several hundred microns from the craze tip. Each sample was strained to similar strains of 0.8%. Micrographs (a), (b) and (c) were strained at $\dot{\epsilon}$ = 0.002, 0.02 and 0.2 in./ min. respectively. It appears that an increase in strain rate produces a decrease in both W_f (final craze width) and the midrib width. However, a fine fibrillar structure is still observed in the midrib region. A clearer understanding of how the midrib region changes with strain rate can be gained from a plot of midrib width/W_f vs strain rate (Figure 8).

Figure 8 shows that the width of the midrib decreases linearly with increasing strain rate. It appears that high strain rates localized deformation near the center of the craze. Also, craze density was found to increase with increasing strain rate. Stress-strain curves for quenched samples at $\dot{\varepsilon}$ = 0.2 in./min. resembled those of annealed samples at $\dot{\varepsilon}$ = 0.02 in./min. (Figure 4). We have found that the morphology of crazes for quenched material at high strain rate is similar to the morphology of the crazes for annealed material at low strain rate. Therefore the mechanical behavior is determined by craze morphology.

After straining to 0.8%, samples with gold mesh were examined in the electron microscope. Figure 9(a) and (b) shows electron micrographs in the mature region several hundred microns from the craze tip of a single craze that was propagated through the tilt edge of a gold shadowed region. Micrograph (c) of Figure 9 was in a region approximately 40μm from the craze tip. Micrograph 9(a) was obtained from an annealed film while micrographs 9(b) and 9(c) were obtained from quenched films.

The resemblance of Figure 9(a) to Figure 9(b) suggests that these crazes developed similarly. It is also interesting to note that the gold particles within both crazes separated from each other in a similar fashion. They appear to form layers parallel to the craze boundary. From measurements of Δ, ϕ and W_f for each craze, W_o, $\bar{\varepsilon}_c$ and $\bar{V}_f$ were calculated. The results of these calculations are summarized in Table 1 for the two specimens differing only in thermal history. Crazes in both

Table 1 - Thermal History Effect on Crazing Parameters for Quenched Thin Films of PS

	ϕ	$\Delta(\mu)$	$W_o(\mu)$	$W_f(\mu)$	$\bar{\varepsilon}_c$	$\bar{V}_f$
annealed*	47°	.57	.61	1.71	1.03	.36
Quenched*	43°	.64	.60	1.68	1.03	.36
Quenched**	43°	.39	.36	1	1.02	.36

* Micrograph in mature region far removed from craze tip.
** Micrograph ∿38μ near craze tip.
ε=0.76% $\dot{\varepsilon}$=.02 in./min.; t=2.3μ

quenched and annealed films had approximately equal values of W_o and W_f. The thermal history did not alter W_o, $\bar{\varepsilon}_c$ or $\bar{V}_f$. At equal strain, the stress for the annealed specimens was considerably larger than that for the quenched specimens (Figure 4). It can be seen that W_o for the micrograph in Figure 9(b) is almost twice as large as that in Figure 9(c). This evidence suggests that as the craze thickens by fibril extension, material is also drawn into the craze from the craze matrix interface.

4. DISCUSSION

4.1 Basic Model

We base our interpretation of the data presented in this paper and in reference [12] on the concept of sequential incorporation of thin layers of material into craze zone. Figure 10(a), (b) depicts two stages of craze development at the craze tip. The first stage is the plastic deformation of a layer of material (Figure 10a). In the second stage, the adjacent layers deform plastically somewhere behind the craze tip (Figure 10b). Plastic deformation increases gradually as the distance from the tip increases.

The layers above and below a deformed layer can be involved in deformation only if sufficient tension exists. Strain hardening and stress concentration for a microelement of volume are necessary to provide the sufficient tension. At present, we do not have experimental data giving the

relationship between stress (σ) and strain (ε) for a microelement of volume. Since the microdiagram should reflect some features of the macrodiagram, we have represented it as in Figure 11. Naturally, the stiffness of the inelastic region at any point is less than the stiffness of the elastic region.

Strain hardening and a higher level of deformation behind the craze tip provide the picture of stress distribution shown in Figure 10(a). Stress concentration does not only occur at the tip of the craze, but also somewhere behind, where the stress can exceed the average (nominal) level. Plastic deformation of the adjacent layers starts at this region of concentration.

4.2 The Concept of Relative Strain Rate

We have assumed a constant strain rate for the microvolume stress-strain curve. The conventional tensile experiment maintains a constant rate of absolute elongation. After the crazes form, all deformation concentrates inside the crazes. If the craze density is constant during the experiment (which is close to experimental evidence), then the absolute elongation of one craze is approximately constant. However, it follows from the scheme of sequential involvement of layers that the rate of relative strain (localized within the craze) must change during the deformation. Assume the thickness of a layer to be 0.01 of W_o. If the relative rate of strain when only the first layer deforms is unity, then Figure 12 represents the change of the average relative strain

rate. Note, that the relative strain-rate changes dramatically when the craze is rather thin. W_o is on the order of 0.1 - 1 μm. Therefore, the rate of the relative deformation may decrease many times during craze deformation. Subsequently, the process of craze formation proceeds with a decreasing relative strain rate, in spite of the fact that a constant strain rate is maintained by the testing machine. It should be noted that the above consideration holds for an average relative strain rate along the craze width.

4.3. Relative Strain Rate and Craze Morphology

Our experimental results show that at sometime during the tensile experiment, flow of additional material into the craze ceases. A straight, sharp boundary between elastically and inelastically deformed material is typical for a mature craze. Our concept of decreasing relative strain rate within the craze explains the restricted incorporation of additional material, and consequently the limited final craze width. The mechanical resistance of a microelement of material should be lower at relative low strain rate than at high strain rate. We can conclude that at some moment during the deformation process the force produced by a deformed element is not enough to involve new material. At this moment, all deformations concentrate inside the craze.

Figure 12 shows that the first layers involved in craze formation deform at a relative high strain rate. Most of the

craze development involves layers which deform at much lower strain rates. The structure of the internal layers may be changed by the destructive process at high strain rate. Tension causes more plastic deformation in the internal layers than in the rest of the layers. Extensive plastic deformation can occur in the internal layers thus producing the distinctive mid-rib.

4.4. Thermal History and Craze Morphology

Figures 4(a,b) present the thermal history and average strain rate effects on mechanical properties of polystyrene. Annealing produces a more dense intermolecular chain packing than quenching. Plastic deformation, due to a nondestructive process, can be produced more easily in quenched films than in annealed films, other conditions being equal. The relative strain rate experienced in the crazed material can cause destructive deformation in annealed films (midrib) and nondestructive in quenched films (no midrib). A manifestation of this morphological difference is the difference in ductility between annealed and quenched samples at strain rate 0.02 in/min. (see Figure 4). The morphological difference can also explain the variation in ductility among the quenched and annealed specimens at different strain rates.

5. CONCLUSIONS

The macro-mechanical properties of thin films of polystyrene are strongly affected by thermal history. The yield

level is higher for annealed than for quenched films, all other conditions being equal. Both annealed and quenched films become more ductile with decreasing average strain rate. At the micro-level, thermal history affects the response of a microvolume of material to local strain rates, which also affects craze morphology and the localized mechanical resistance.

Studies using high resolution electron microscopy showed the relationships between craze morphology and the observed ductility. Brittle behavior is always observed in samples with voiding midribs in the craze. As a craze thickens by fibril extension, material is simultaneously drawn into the craze from the craze-matrix interface. Strips of material are drawn into the craze until at some critical point drawing stops and the craze thickens only by fibril extension.

The proposed theory explains the mechanism by which a craze develops in width, including the formation of the boundary and the midrib zone. The assumption of a large decrease in local relative strain rate, as the craze widens, is the key factor in our explanation.

ACKNOWLEDGMENT

The authors wish to thank the Office of Naval Research for its generous financial support of this work. We would like to thank also Dr. Rowan Truss and Dr. Stephen Wellinghoff for their stimulating discussions and helpful suggestions.

REFERENCES

1. S. RABINOWITZ and BEARDMORE, CRC Crit. Reviews in Macromol. Sci. Vol. 1 (edited by E. Baer, P. Geil and J. Koenig) Cleveland: CRC Press (1972) 1.

2. R. P. KAMBOUR, J. Polym. Sci. Macromol. Rev. 7 (1973) 1.

3. A. N. GENT, J. Mater. Sci. 5 (1970) 925.

4. S. S. STERNSTEIN and L. ONGCHIN, Poly. Prepr. 10 (1969) 117.

5. K. C. RUSCH and R. H. BECK, jr., J. Macromol. Sci-Phys. B3 (3) (1969) 365, B4 (3) (1970) 261.

6. R. N. HAWARD, Amorphous Materials (R. W. Douglas and B. Ellis, Eds.) London (1972) 513.

7. E. H. ANDREWS and S. BEVAN, Polymer 13 (1972) 337.

8. A. S. ARGON, J. Macromol. Sci. Phys. (B 8) (1963) 573.

9. S. WELLINGHOFF and E. BAER, J. Macromol. Sci. -Phys. B11 (3) (1975) 367.

10. H. G. OLF and A. PETERLIN, J. of Polym. Sci. A-2 12 (1974) 2209.

11. P. BEAHAN, M. BEVIS and D. HULL, J. Mater. Sci. B (1972) 162.

12. E. J. KRAMER, "Environmental Cracking of Polymers", to appear in Developments in Polymer Fracture, ed. by E. H. Andrews, Applied Science Publishers, Ltd. 1979.

13. N. VERHEUPEN-HEYMANS and J. C. BAUWENS, J. of Mat. Sci. 11 (1976) 7.

14. S. TOLANSKY, Multiple-beam Interferometry of Surfaces and Films, Clarendon Press, Oxford (1948).

15. L. E. NIELSON, "Mechanical Properties of Polymers", Reinhold, New York (1962) 131.

16. P. BEAHAN, M. BEVIS and D. HULL, Proc. R. Soc. Land. A343 (1975) 525.

FIGURE CAPTIONS

1. (a) Geometry of thin film polystryene specimen; all are in inches.
   (b) Optical photograph of a gold shadowed grid on the surface of a specimen. The arrow indicates direction of applied stress.
   ε=0.76%; $\dot{\varepsilon}$=0.02 in./min.; t=2.4μm
2. A scheme of crack propagation through tilt edge of a shadowed zone: (a) Before stress is applied, (b) after stress is applied; the large arrows indicate direction of applied stress.
3. A scheme of craze propagation through tilt edge of a shadowed zone: (a) Before stress is applied, (b) after stress is applied; the large arrows indicate direction of applied stress.
4. Stress-strain curves as a function of strain rate for (a) annealed and (b) quenched thin-film PS specimens in tension. All strain-rates are given in in./min.
5. Optical photographs of gauge area for quenched thin-film PS specimen with: (a) parallel polarizers, (b) crossed polarizers. Arrow indicates direction of applied stress. ε=2.8%; $\dot{\varepsilon}$=0.02 in./min.; t=2.7μm.
6. Electron micrographs of a typical craze, formed in (a) annealed and (b) quenched specimens at $\dot{\varepsilon}$=0.02 in./min. The micrographs were taken after fracture. The arrow indicates direction of applied stress and distance M-M

defines the thickness of midrib.

7. Electron micrographs showing strain-rate effect on craze morphology in quenched thin-film PS specimens: (a) $\dot{\varepsilon}$=0.002 in./min., (b) $\dot{\varepsilon}$=0.02 in./min., (c) $\dot{\varepsilon}$=0.2 in./min. Arrow indicates direction of applied stress. All specimens were strained to ε=0.76%, with t=2.4μm.

8. Plot of midrib width/craze width vs. strain-rate showing effect of strain-rate on midrib for quenched P.S. specimens.

9. Electron micrographs of a section of a craze propagated through tilt edge of a gold shadowed zone: (a) annealed specimen (b) quenched specimen, (c) quenched specimen 40 μm near craze tip. Arrow indicates direction of applied stress.
ε=0.76%; $\dot{\varepsilon}$=0.02 in./min.; t=2.3μm.

10. Two stages of craze development at a craze tip: (a) Plastic deformation of a layer and relevant stress distribution along the layer; (b) Start of plastic deformation of the adjacent layers. The shaded regions indicate plastically deformed material.

11. Assumed stress-strain diagram for microvolume of the material.

12. (a) Three stages of craze widening showing the change in length over which plastic deformations occur.
(b) Dependence of relative strain rate on relative thickness of craze at constant average strain rate.

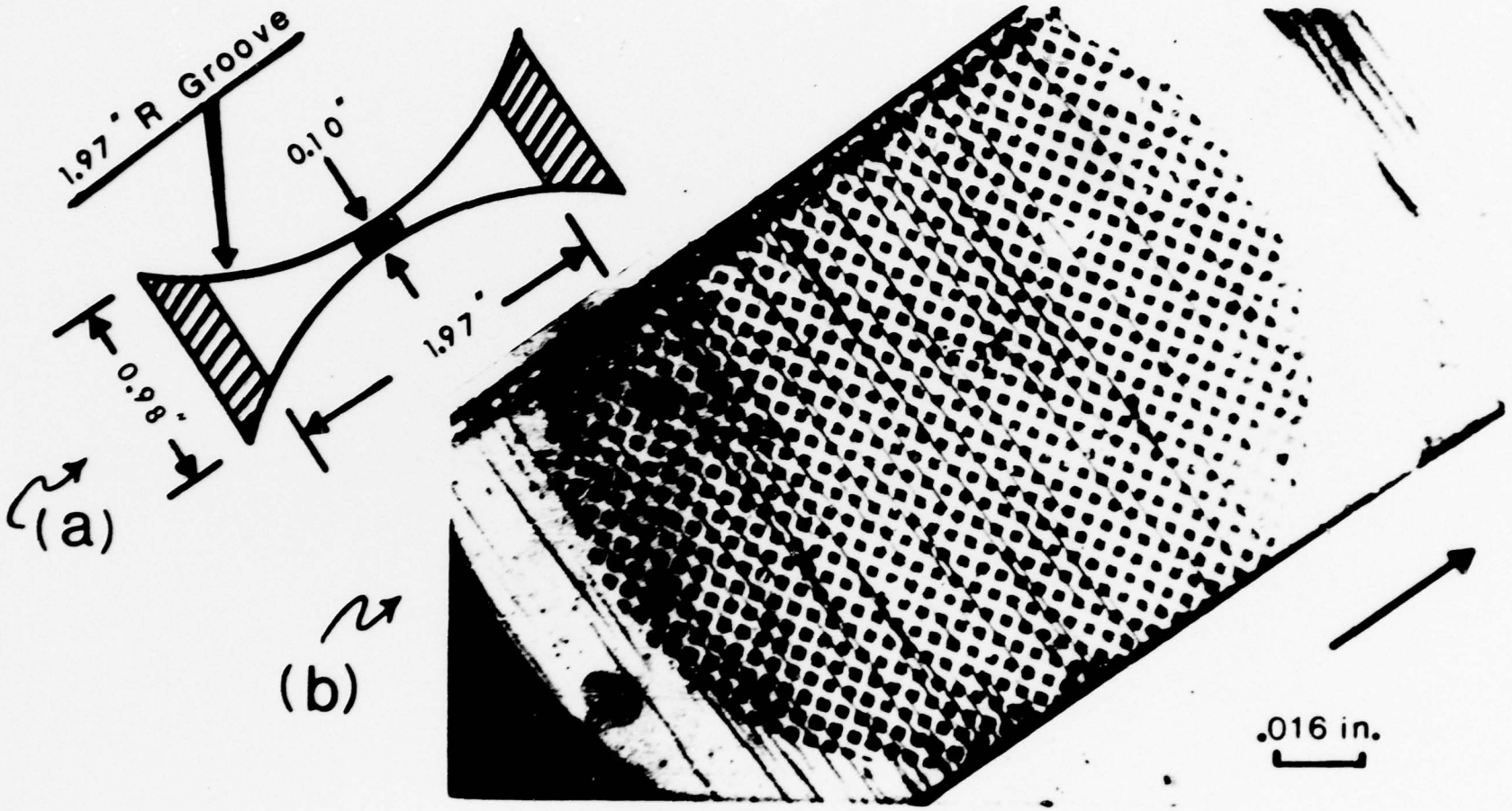
1.97" R Groove
0.10"
1.97"
0.98"
(a)
(b)
.016 in.

Crack Propagation Through Tilt Edge of Shadowed Zone

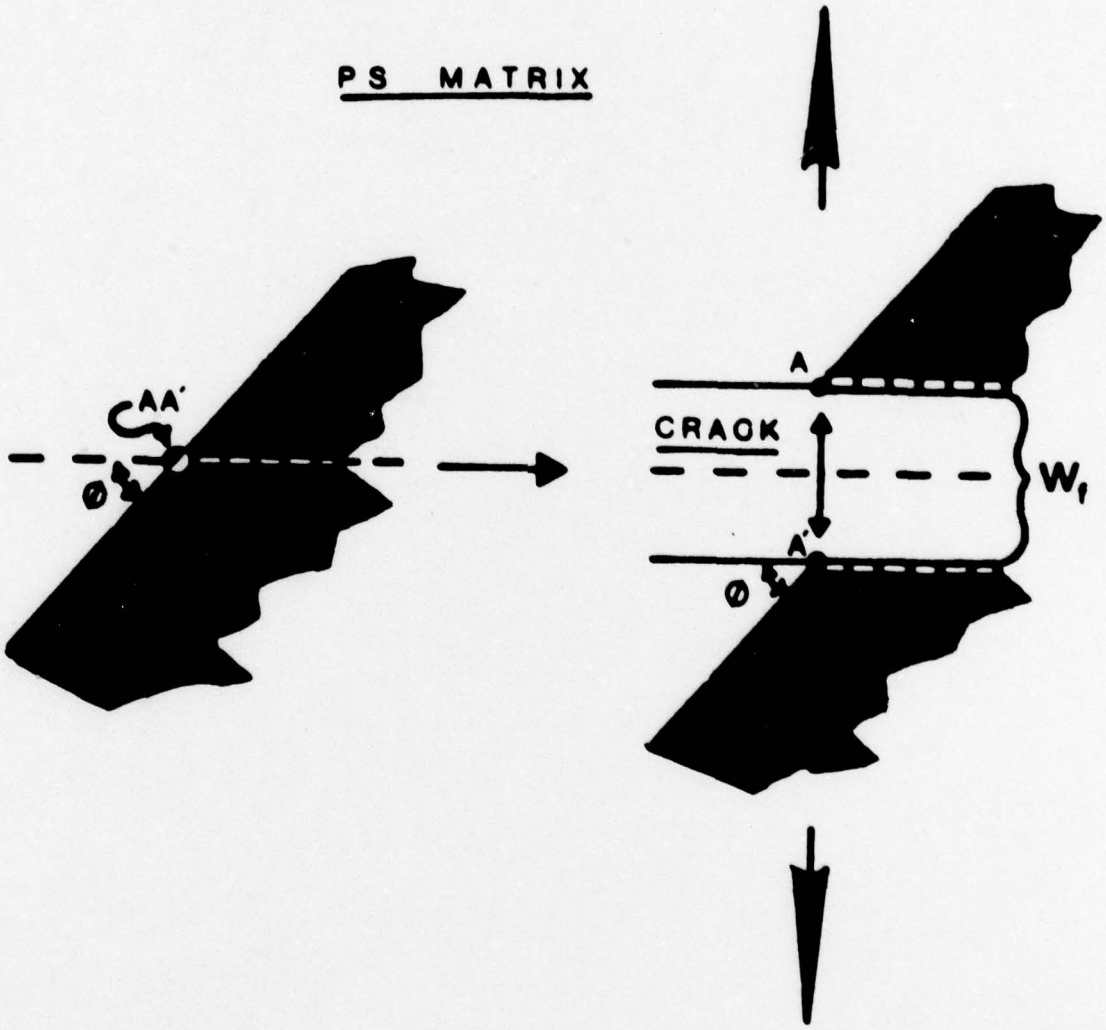

Craze Propagation Through Tilt Edge of Shadowed Zone

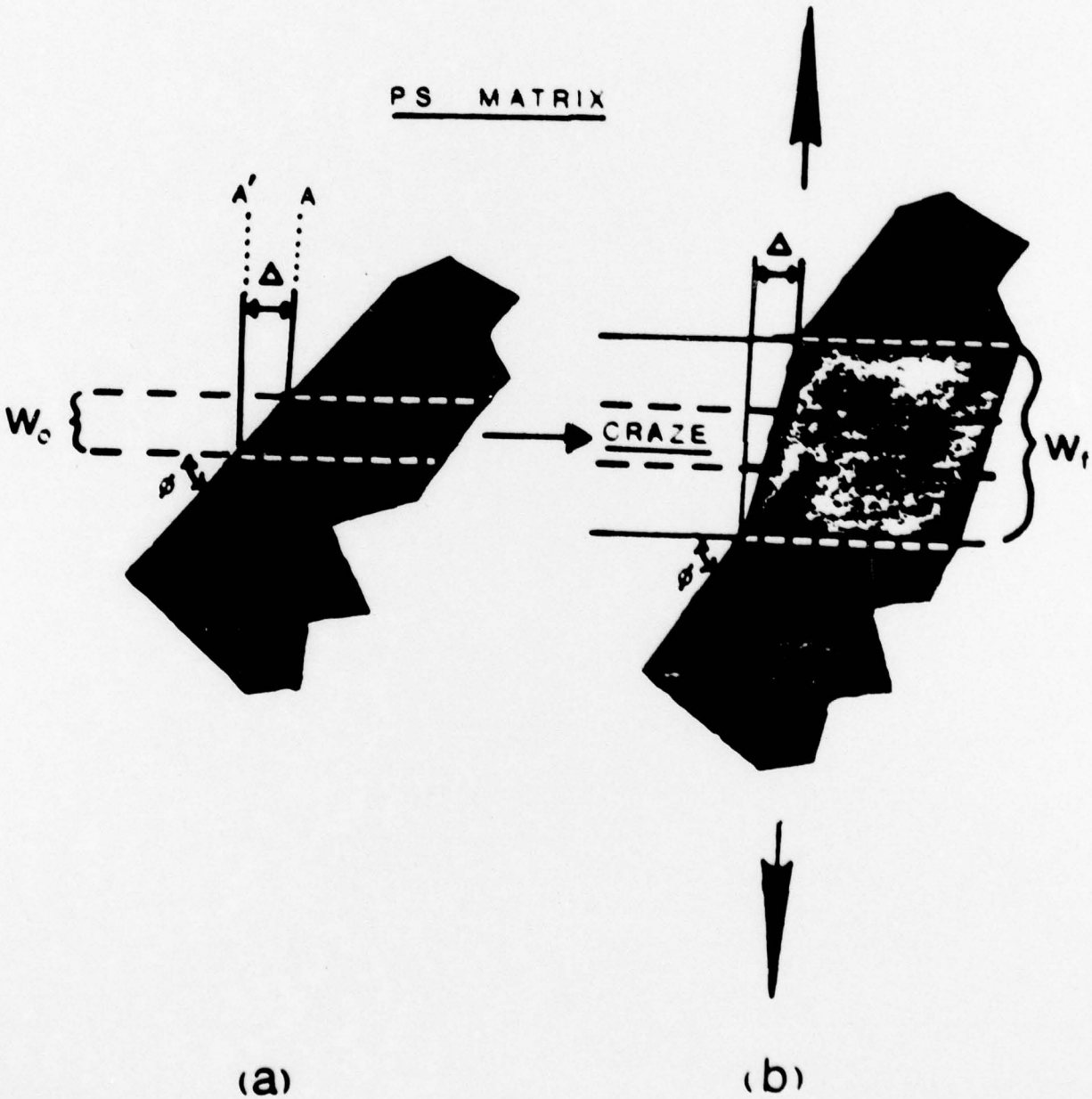

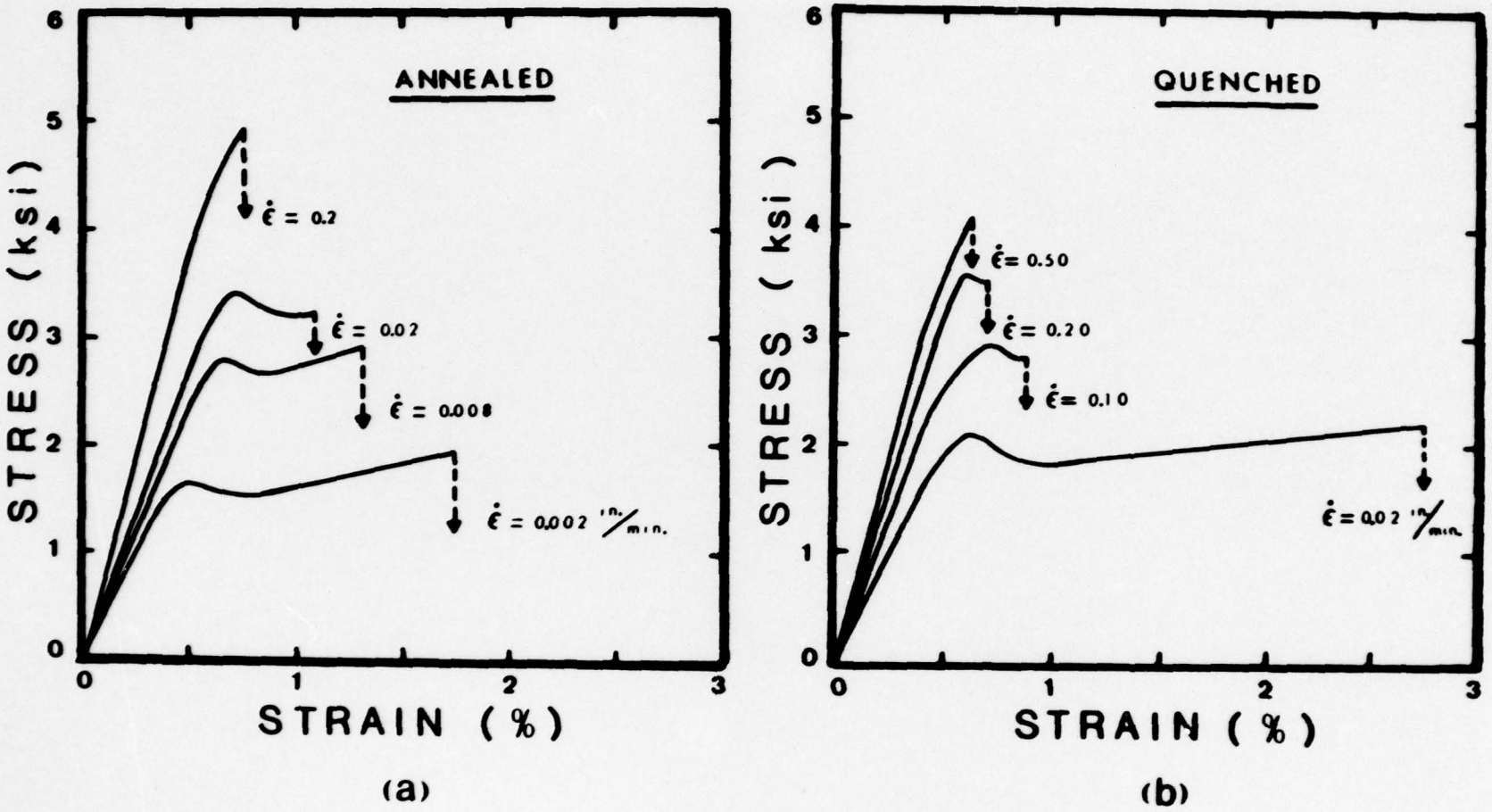
ANNEALED
STRESS (ksi)
STRAIN (%)
$\dot{\epsilon}$ = 0.2
$\dot{\epsilon}$ = 0.02
$\dot{\epsilon}$ = 0.008
$\dot{\epsilon}$ = 0.002 in./min.
0
1
2
3
4
5
6
(a)
QUENCHED
STRESS (ksi)
STRAIN (%)
$\dot{\epsilon}$ = 0.50
$\dot{\epsilon}$ = 0.20
$\dot{\epsilon}$ = 0.10
$\dot{\epsilon}$ = 0.02 in./min.
(b)

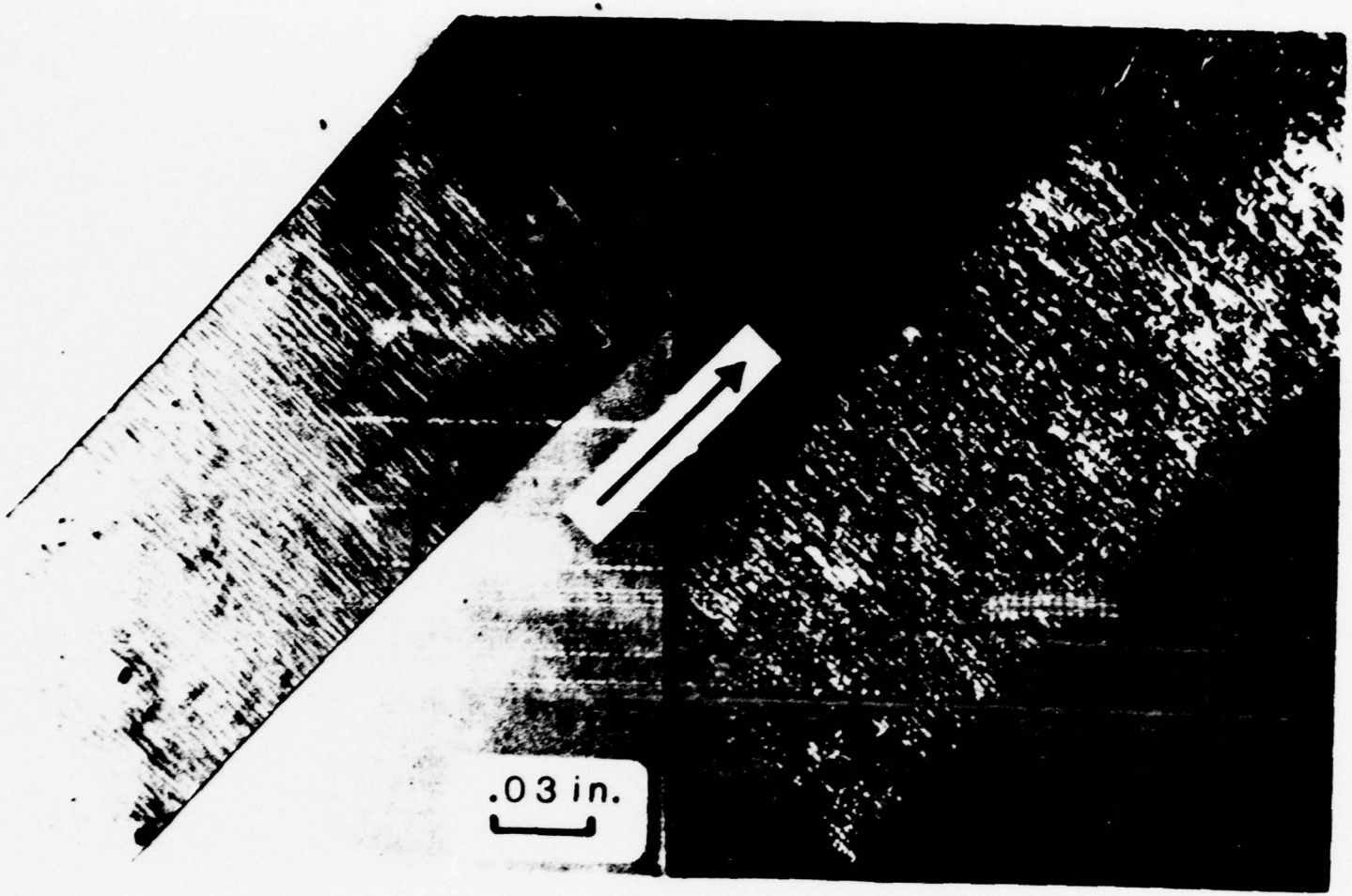

(a) (b)

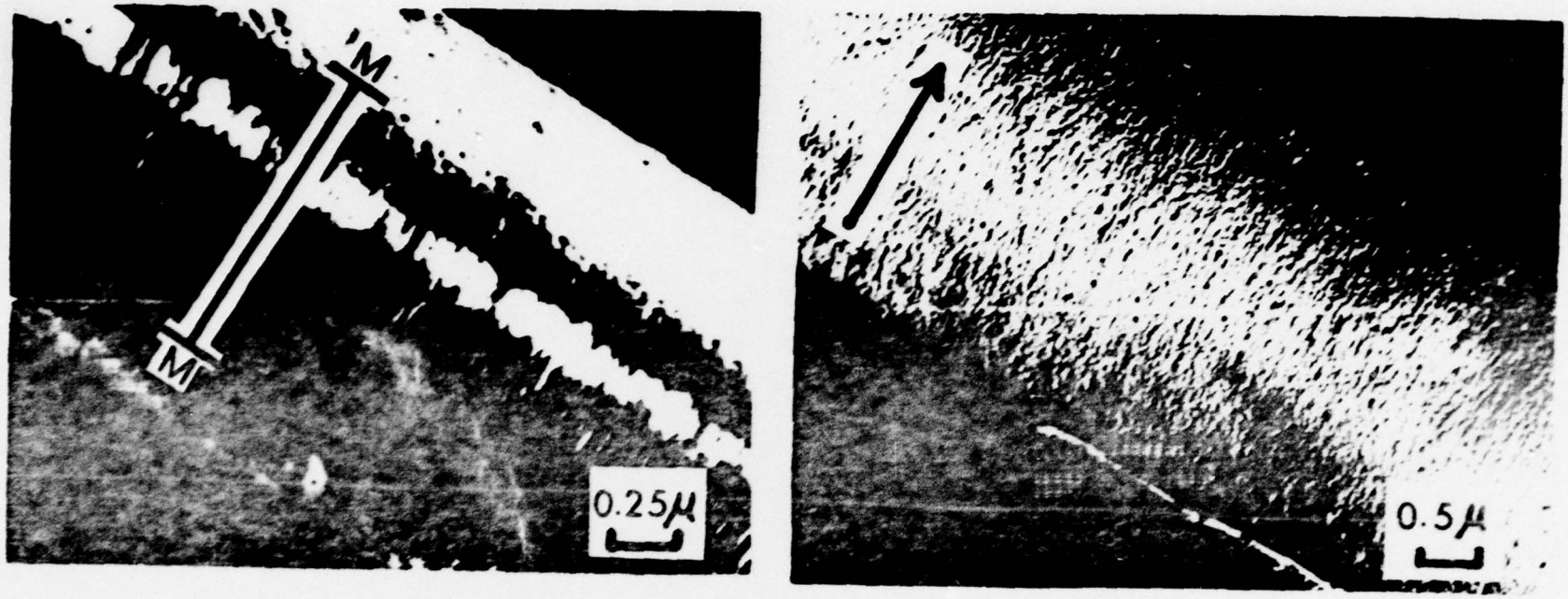

(a)

(b)

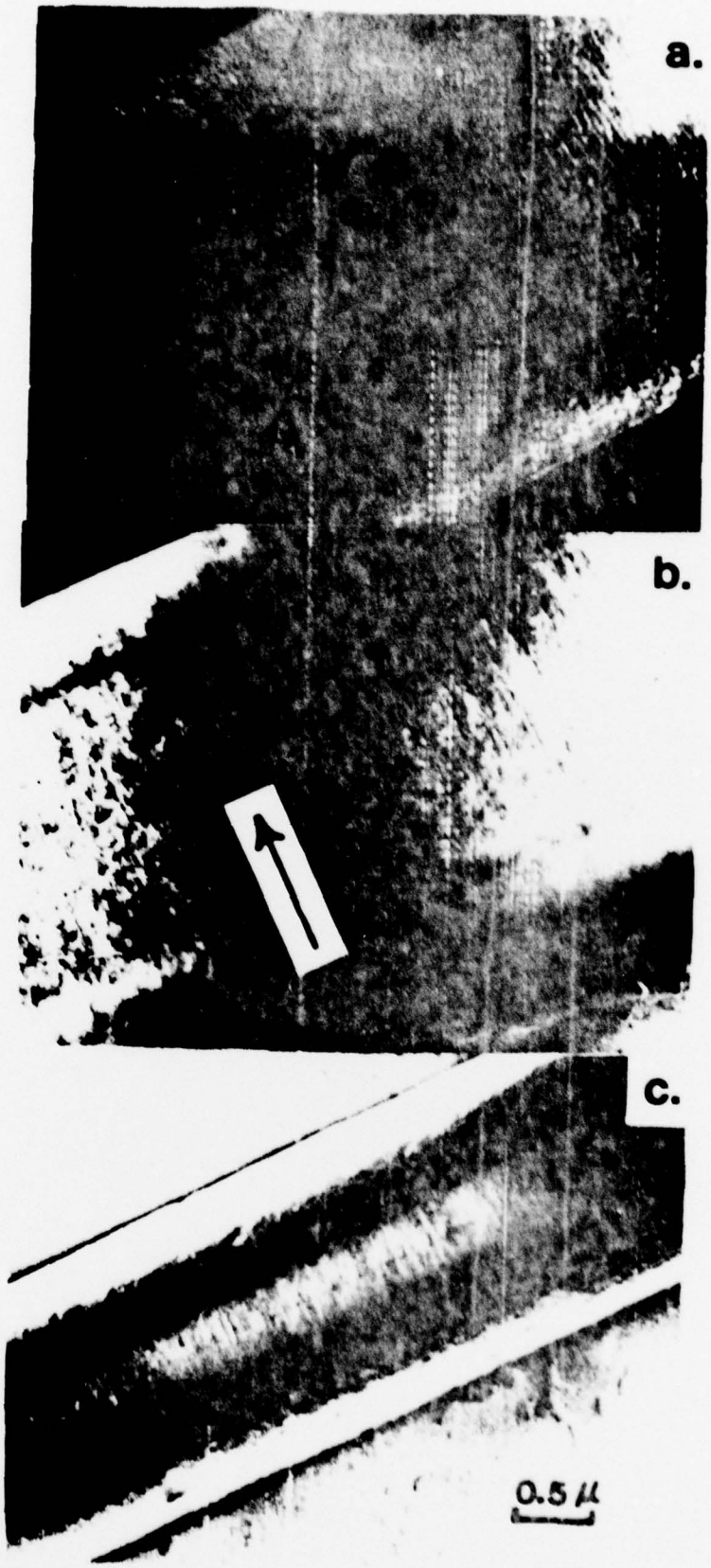
a.
b.
c.
0.5 μ

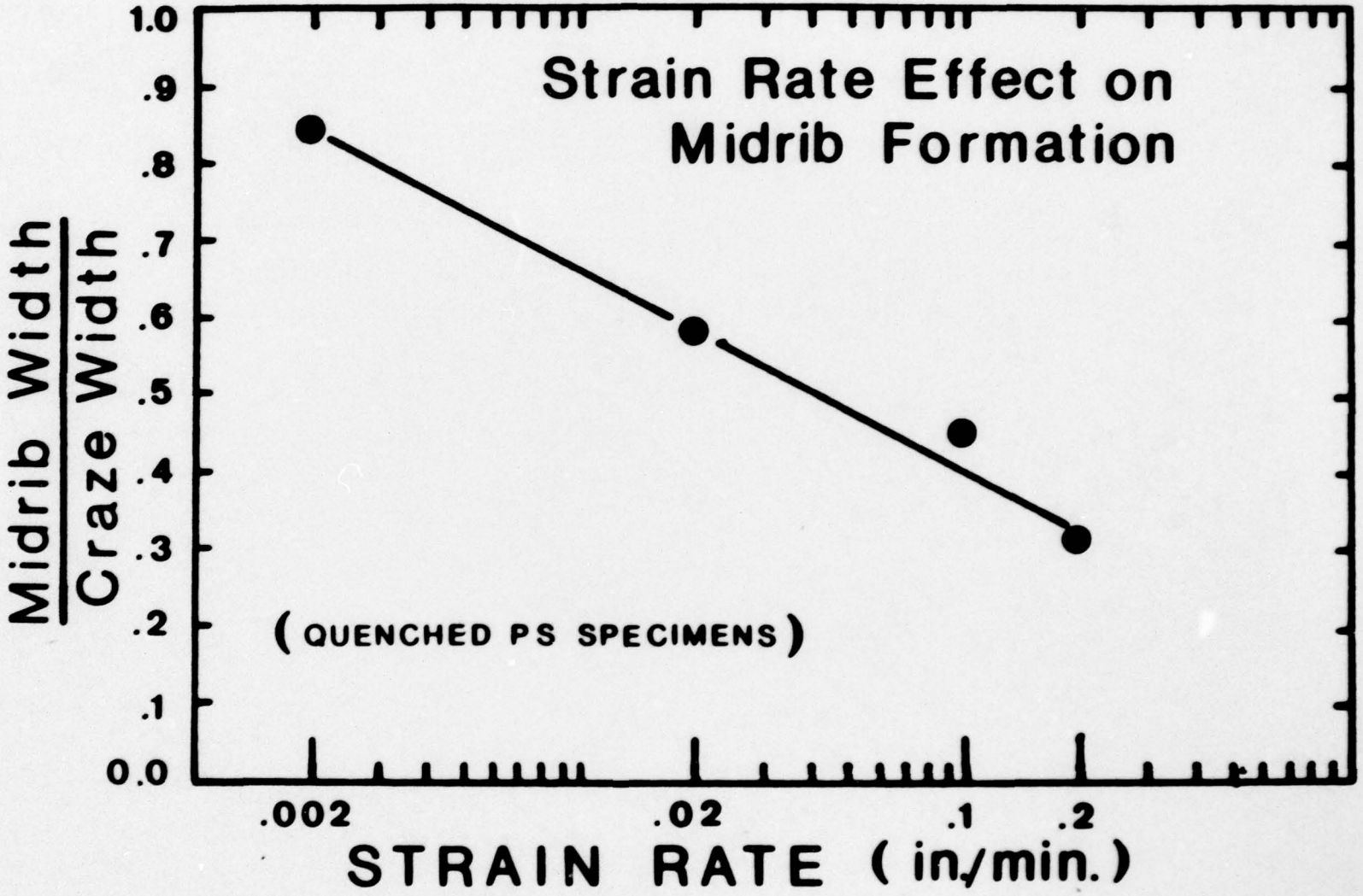
Strain Rate Effect on
Midrib Formation
Midrib Width / Craze Width
1.0
.9
.8
.7
.6
.5
.4
.3
.2
.1
0.0
(QUENCHED PS SPECIMENS)
.002
.02
.1
.2
STRAIN RATE (in/min.)

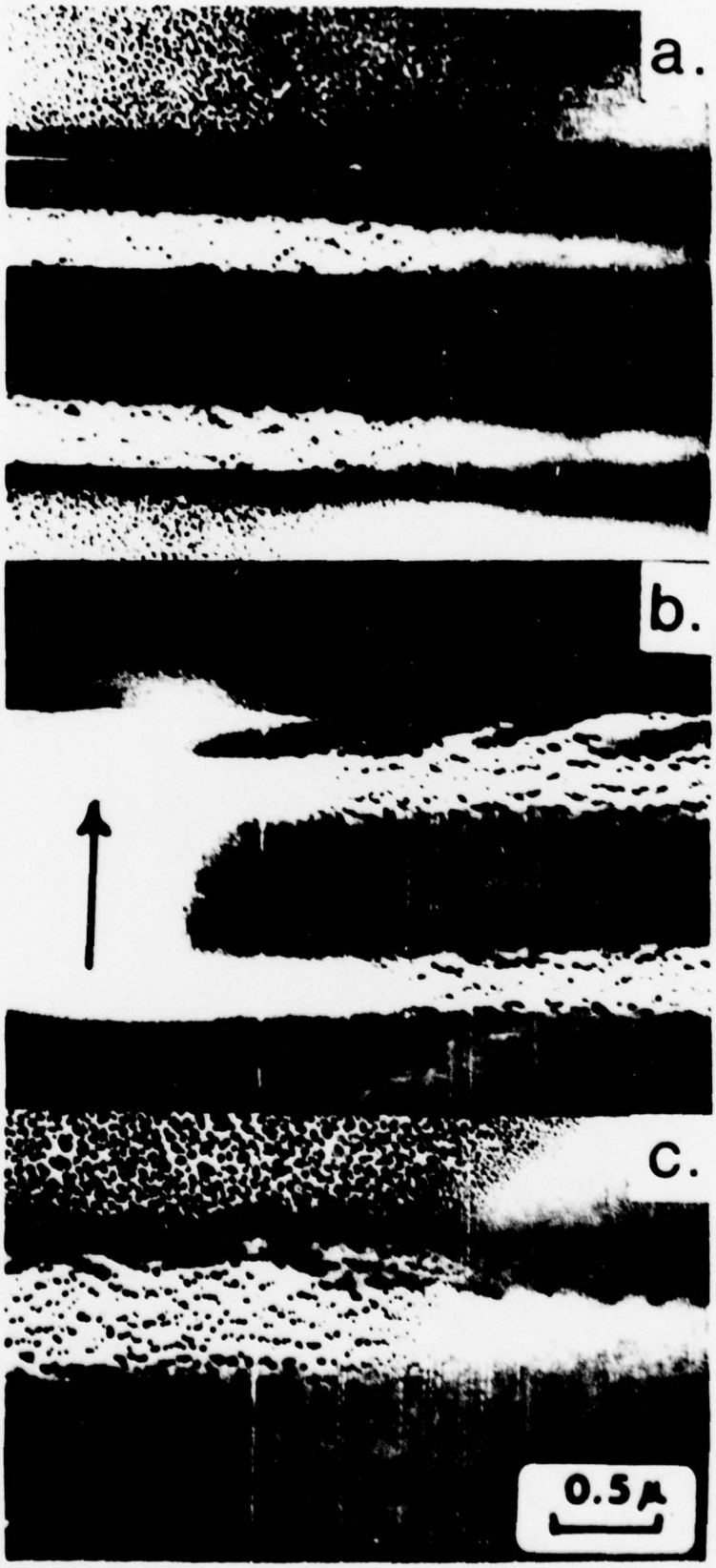
a.
b.
c.
0.5 μ

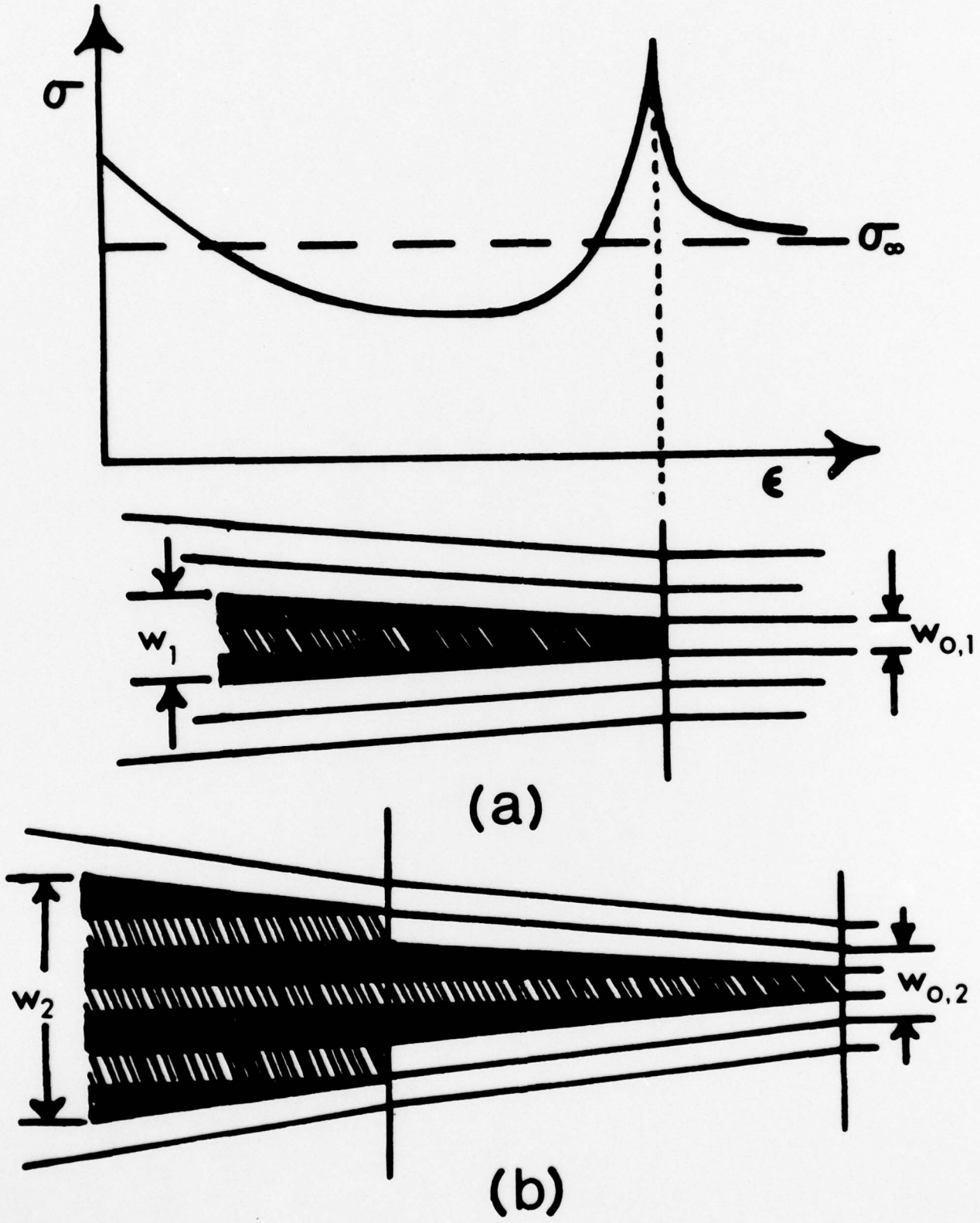
σ
σ∞
ε
w1
wo,1
(a)
w2
wo,2
(b)

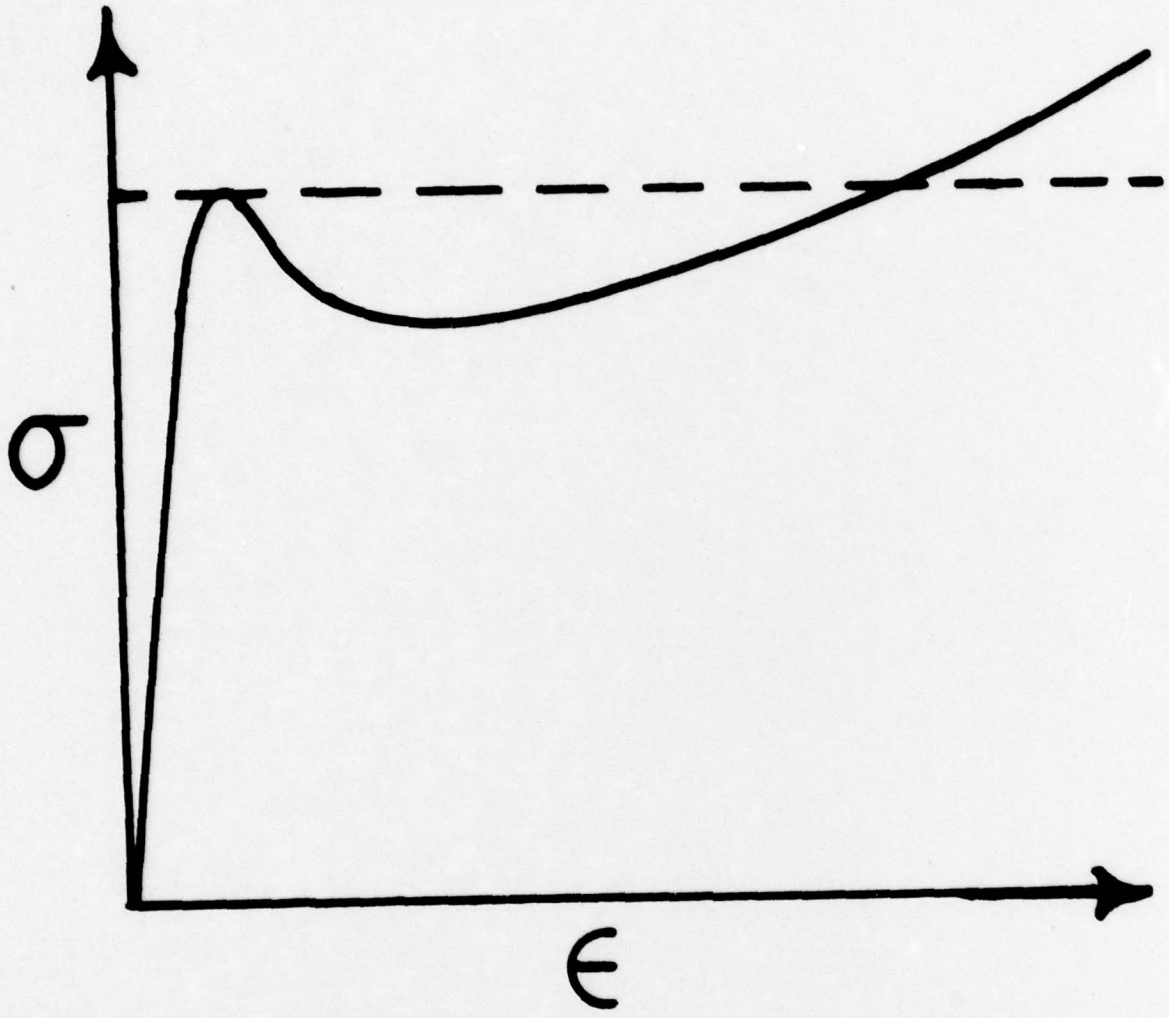
σ
ϵ

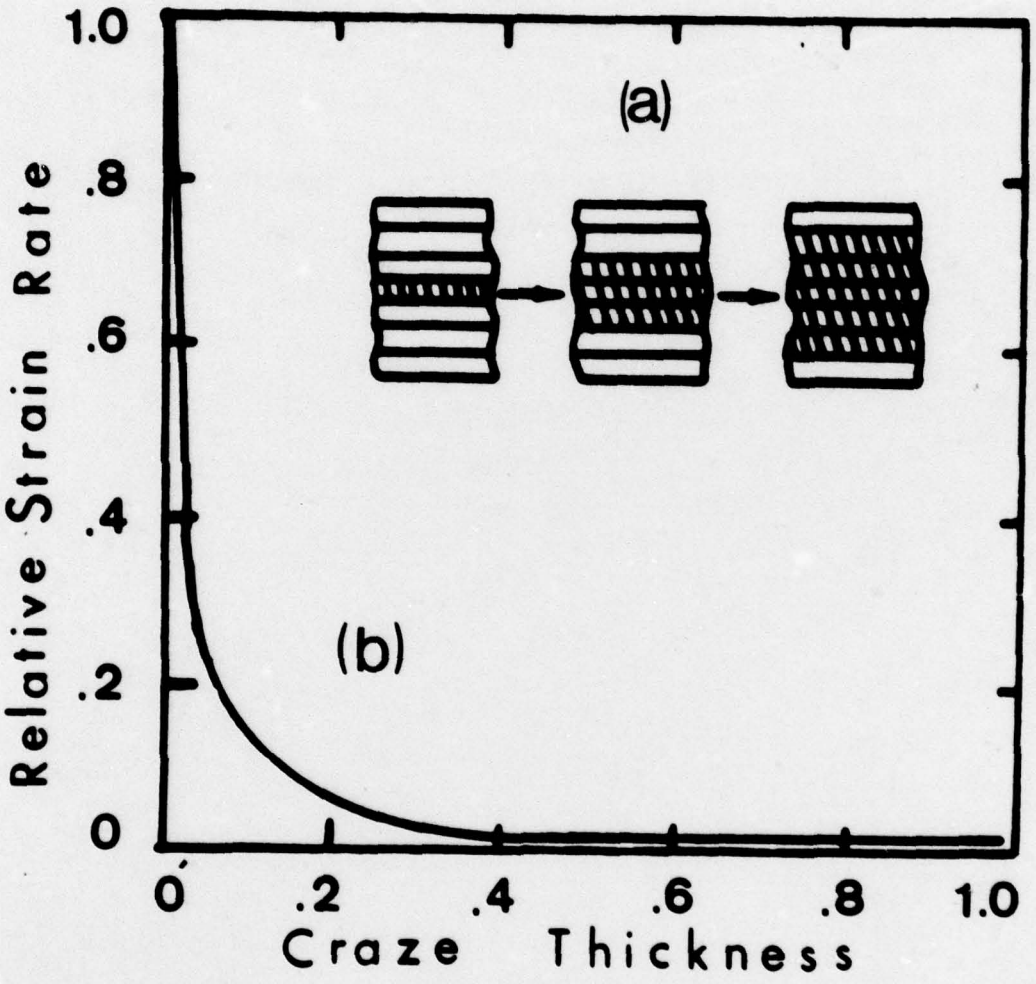
1.0
.8
.6
.4
.2
0
Relative Strain Rate
(a)
(b)
0
.2
.4
.6
.8
1.0
Craze Thickness